Biochimica et Biophysica Acta 857 (1986) 146–154
Elsevier

BBA 73096

The kinetics of glucose transport in human red blood cells

Allan G. Lowe and Adrian R. Walmsley

Department of Biochemistry, Medical School, University of Manchester, Manchester, M13 9PT (U.K.)

(Received December 24th, 1985)

Key words: Glucose transport; Kinetics; (Erythrocyte membrane)

A quenched-flow apparatus and a newly developed automated syringe system have been used to measure initial rates of D-[^{14}C]glucose transport into human red blood cells at temperatures ranging from 0° to 53°C. The Haldane relationship is found to be obeyed satisfactorily at both 0 and 20°C, but Arrhenius plots of maximum D-[^{14}C]glucose transport rates are non-linear under conditions of both equilibrium exchange and zero trans influx. Fitting of the data by non-linear regression to the conventional model for glucose transport gives values at 0°C of $0.726 \pm 0.0498\ s^{-1}$ and $12.1 \pm 0.98\ s^{-1}$ for the rate constants governing outward and inward movements of the unloaded carrier molecule and $90.3 \pm 3.47\ s^{-1}$ and $1113 \pm 494\ s^{-1}$ for outward and inward movements of the carrier-glucose complex. Activation energies for these four rate constants are respectively 173 ± 3.10, 127 ± 4.78, 88.0 ± 6.17 and $31.7 \pm 5.11\ kJ \cdot mol^{-1}$. These parameters indicate that at low temperatures the marked asymmetry of the transport mechanism arises mainly from the high proportion of inward-facing carriers and carrier-glucose complexes, and that there is a relatively small difference between the affinities of the carrier for glucose in the inward and outward-facing conformations. At high (physiological) temperatures the carrier is fairly evenly distributed between outward- and inward-facing conformations and the affinity for glucose is about 2.5-times greater outside than inside.

Introduction

The glucose carrier of the human red blood cell is one of the most intensively studied transport systems, with isolation of the carrier molecule [1], specific labelling with cytochalasin B [2] and fluorescence studies of single half turnovers [3] among recent interesting advances. The amino-acid sequence and trans-membrane disposition of the glucose carrier in human hepatoma cells has also been determined [4]. Despite this progress, the essential kinetics of the transport mechanism remain only partially resolved. Most kinetic studies have involved measurements of isotope-labelled glucose exchange under equilibrium exchange conditions, or net movement of glucose under 'infinite-cis' or 'infinite-trans' conditions, but studies of glucose entry into glucose-free cells have been few and restricted to relatively low temperatures, while only Brahm [5] and Miller [6] have measured initial rates of glucose efflux from cells in to glucose-free medium. The rapidity of glucose transport has also restricted most studies to well below the physiological temperature range.

In this work, we describe the application of a recently developed rapid reaction technique [7] and a newly developed semi-rapid reaction technique to measurements of glucose transport in human red cells under conditions of equilibrium exchange entry and zero trans entry and exit, at temperatures between 0 and 53°C. This work has enabled us to characterise the transport mecha-

Abbreviations: maximum rates of transport under conditions of equilibrium exchange, zero trans influx and zero trans efflux are respectively V^{ee}, V_{oi}^{zt}, and V_{io}^{zt}. Michaelis constants (K_m) under conditions of equilibrium exchange, zero trans influx and zero trans efflux are respectively K^{ee}, K_{oi}^{zt}, and K_{io}^{zt}.

nism in terms of the rate constants for reorientation of the free and glucose-loaded carrier across the membrane and the dissociation constants for glucose of the inside- and outside-facing carrier.

Materials and Methods

Solutions

Citrate-phosphate-dextrose: 3.2 g citric acid, 25.8 g trisodium citrate, 21.8 g sodium dihydrogen phosphate, 25 g D-glucose in 1 litre distilled water. Isotonic saline: 165 mM NaCl. Isotonic phosphate: 110 mM disodium hydrogen phosphate adjusted to the required pH with 165 mM sodium dihydrogen phosphate. Phosphate-buffered saline: 80 parts isotonic saline and 20 parts isotonic phosphate. Quench solution: 150 μM phloretin and 10 μM mercuric chloride in phosphate-buffered saline (pH 6.0), made up immediately before use. Drabkin's solution: 1 g $NaHCO_3$, 50 mg KCN and 200 mg $K_3Fe(CN)_6$ in 1 litre distilled water. Glucose solutions were prepared in phosphate-buffered saline (pH 7.4) with or without addition of D-[U-^{14}C]glucose (0.1 μCi/ml) as tracer.

Preparation of erythrocytes

Freshly collected blood from polycythemic patients was mixed with citrate-phosphate-dextrose (5 : 1, v/v) and stored at 4°C before use within 7 days. Red blood cells were collected by centrifugation and after removal of plasma cells were washed four times with 10 vol. isotonic saline to remove both intra- and extracellular glucose.

Procedures for flux measurements

(i) Zero trans influx. 1.5 ml isotonic phosphate-buffered saline containing D-[^{14}C]glucose at the required concentration was rapidly added to 100 μl glucose-free red blood cells at about 50% haematocrit. After the required incubation time, influx of D-[^{14}C]glucose (which was always less than 10% of the extent of uptake at equilibrium) was stopped by addition of 5 ml ice-cold 150 μM phloretin/10 μM $HgCl_2$. The cell suspension was immediately centrifuged at $3500 \times g$ for 1 min, after which the supernatant was removed by aspiration and the cells were washed by resuspension and recentrifugation in a further 5 ml phloretin/$HgCl_2$ solution. Sedimented cells were then haemolysed with 1 ml water and (after removal of 0.1 ml for analysis of haemoglobin) proteins were precipitated by addition of 0.1 ml 100% (w/v) trichloroacetic acid and sedimented by bench centrifugation. 0.6 ml of the supernatant was taken for assay of D-[^{14}C]glucose by scintillation counting. Haemoglobin was assayed by mixing 0.1 ml haemolysed cell suspension with 3.0 ml Drabkin's solution then measuring absorbance at 540 nm 30 min later. This procedure was used for both manual mixing experiments (incubation times of 10 s or longer) and with the automated syringe system described below, with which incubation times as short as 0.25 s were possible. At high temperatures, when incubation times of less than 0.2 s were necessary, the quenched flow method described by Lowe and Walmsley [7] was used. This is essentially similar to the above procedure, except that the ratio of the volume of cell suspension to the volume of D-[^{14}C]glucose solution was 1 : 6 in typical quenched-flow experiments.

The rate of glucose transport was calculated from radioactivity incorporated into the cell extract on the basis that the mean cell haemoglobin content was 29 pg/cell, that there were 1.8 litre cell water per kg haemoglobin and $3.1 \cdot 10^{13}$ cells per litre cell water. Rates calculated (mmol/litre cell water per s) agreed well with calculations based on 100% filling of the cells with radioactivity, and all the cell water appeared to be available to glucose.

(ii) Equilibrium exchange influx. These experiments were carried out as for zero trans influx, except that the red blood cells were pre-equilibrated with unlabelled glucose at the same concentration as that in the solution of D-[^{14}C]glucose.

(iii) Zero trans efflux. Aliquots of red blood cells were pre-equilibrated with a series of the required concentrations of unlabelled glucose, then tracer D-[^{14}C]glucose was added and incubation continued to allow equilibration of the isotope. (This two-stage equilibration procedure was used to minimize metabolism of D-[^{14}C]glucose during equilibration.) Red blood cells were then collected by centrifugation and efflux experiments were started by adding 1.5 ml phosphate-buffered saline to 10 μl red cells at 80% hematocrit. The remainder of the procedure was as described for zero trans influx.

For all measurements of V_{max} and K_m the range of glucose concentrations used ranged from about $0.1 \times K_m$ to between 5 and $10 \times K_m$.

Automated syringe system

The instrument consisted of two spring-driven syringes, the sequential delivery of which was controlled by an electronic timer (Radio Spares Universal Digital Timer No. 346390, Radio Spares, U.K.) (Fig. 1). In each syringe-drive, the tension in two springs was used to drive a stainless steel plunger, which in turn drove the barrel of a plastic syringe ejecting solution from the syringe into the mixing vessel (usually a 15 ml plastic test-tube). The spring-driven plunger assembly was enclosed in a stainless-steel jacket (dimensions $16.5 \times 2.5 \times 2.5$ cm) with slots running parallel to the plunger on two sides of the jacket. The slots, which acted as a guide for a metal bar fixed at right-angles to the end of the plunger, ended in a recess which served to lock the plunger in position when the springs were tensed. Plunger movement was triggered by a solenoid, placed directly above the recess, which acted by displacing the metal bar. The two spring-driven syringes and solenoids were mounted on a wooden block (dimensions $42 \times 10.5 \times 2$ cm) which was inclined at about 20° from perpendicular during operation.

Short lengths of polyethylene tubing were used to guide the syringe contents to the mouth of the reaction tube, which was supported at an angle of about 20° from vertical so that the syringe contents were delivered down the side of the reaction tube in order to minimise splashing. The syringes were held by metal cradles (retained by screw clamps) the positions of which were adjustable to permit the volumes delivered by the syringes to be varied. Almost any type of commercially available

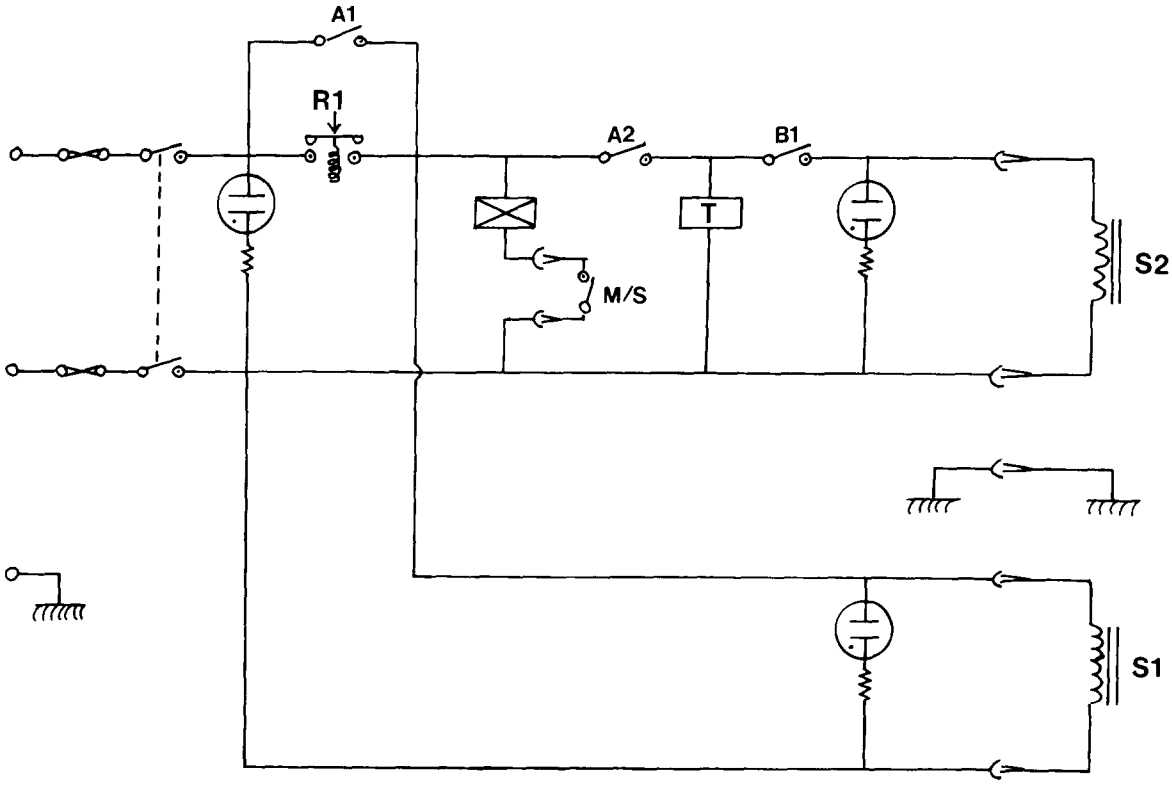

Fig. 1. A circuit diagram of the timing device and solenoids controlling the automated syringe system. The reset switch (R1) closed A1 and A2 and activated solenoid S1 and the timer (T). The timer controlled the delay before closure of B1 and activation of solenoid S2. The microswitch (M/S) cut off power to the solenoids at the time when S2 was activated, and restored power when the syringe-drives were re-loaded.

plastic syringe (volumes between 0.5 and 10 ml) could be used.

The device was operated as follows. One reactant (e.g., 0.1 ml red blood cell suspension) was placed in the reaction tube, one syringe was loaded with the second reactant (e.g., 1.5 ml D-[^{14}C]glucose solution), and the second syringe was loaded with quenching reagent (e.g., 5 ml phloretin solution). Delivery of the first reactant into the reaction tube was initiated by pressing the timer reset switch, which triggered the first solenoid and syringe-drive. The second solenoid drive was then activated automatically after a time delay which could be preset to 10 ms or any longer time. Spring tension in the syringe drives was adjusted to allow delivery of 1 ml reaction medium in less than 50 ms. The syringe-drives were reloaded manually using thumb-presses and the process of reloading reactivated the solenoids ready for re-use.

The whole syringe system was kept in a thermostatically controlled box and additional thermostatic control of the reaction syringe was effected by circulating water through a glass coil surrounding the syringe.

The overall performance of the automated syringe device was assessed by measuring the rate constant for the alkaline hydrolysis of 2,4-dinitrophenyl acetate. In these tests, 0.1 ml 5.2 mM 2,4-dinitrophenyl acetate was placed in the reaction tube and 1.0 ml of 51 mM NaOH was injected into the vessel. The reaction was quenched with 5 ml ice-cold 1 M HCl from the second syringe and 2 M sodium acetate was immediately added to adjust the pH to 4.0. The hydrolysis product (2,4-dinitrophenol) was then assayed by measuring absorbance at 360 nm. This procedure gave a value of 58.2 ± 4.08 $M^{-1} \cdot s^{-1}$ for the second-order rate constant for hydrolysis at 20°C, a value which agrees well with published values [8].

Results and Discussion

Use of our recently developed quenched-flow and automated syringe systems has made it possible to measure initial rates of D-[^{14}C]glucose influx into human red cells at temperatures between 0 and 53°C, and with the ranges of glucose concentration necessary to measure K_m and V_{max} for glucose transport under both zero trans and equilibrium exchange conditions. The new methods were particularly valuable for measurements of zero trans influx, since under this condition large errors can arise from back-flow of radioactive glucose if filling of the cells exceeds 10%. This effect becomes very marked at temperatures exceeding 20°C. The Arrhenius plots in Fig. 2 show that V_{max} for both zero trans and equilibrium exchange influx of D-[^{14}C]glucose are strongly temperature-dependent with activation energies substantially greater below than above about 25°C.

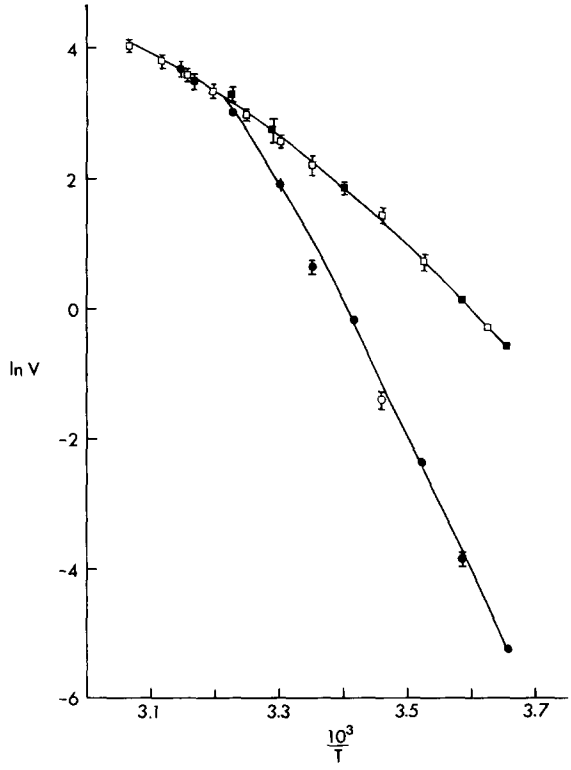

Fig. 2. The temperature dependences of V_{max} for influx of D-[^{14}C]glucose into human red cells under zero trans (●, ○) and equilibrium exchange (■, □) conditions. Solid symbols represent V_{max} determined from experiments at six concentrations of glucose with at least four measurements per concentration. Error bars encompass 2 S.E. Open symbols are V_{max} calculated from measurements made at 264 or 300 mM glucose assuming that K^{ee} is 15 mM at all temperatures: or at 20 mM glucose assuming that K_{oi}^{zt} is 1.2 mM at 16°C. The technique used to measure influx (manual mixing, automated syringe system or the quenched flow apparatus) was selected in order to achieve less than 10% isotopic filling of the cells under all conditions. The lines indicating the theoretical values of V^{ee} and V_{oi}^{zt} were calculated from the parameters listed in Table II.

The actual values of V_{max} indicated in Fig. 2 are broadly in line with previous studies of temperature dependence [5,9,10], but only Lacko et al. [11] have reported such clear-cut biphasic behaviour in their measurements of glucose influx under 'infinite trans conditions'. The way in which these Arrhenius plots can be fitted to the conventional model for glucose transport will be dealt with in the following section, but it is notable that influx under zero trans conditions is clearly more strongly temperature-dependent than that under equilibrium exchange conditions and in consequence the 'trans effect' (the ratio of V^{ee} to V_{oi}^{zt}) also shows a strong temperature-dependence and decreases from just over 100 at 0°C to less than 1.4 at 37°C (Fig. 3).

In contrast to the rates of D-[^{14}C]glucose transport, the temperature-dependences of the K_m for transport are relatively small. Under equilibrium exchange conditions K^{ee} for D-[^{14}C]glucose influx varies only between about 12 and 17 mM, whereas K_{oi}^{zt} increases gradually from about 0.15 mM at 0°C to 19.6 mM at 43°C. Van't Hoff plots for the variation of $\ln(K_{oi}^{zt})$ and $\ln(K^{ee})$ with reciprocal temperature are shown in Fig. 4. The slopes of these indicate apparent enthalpies of 74 kJ · mol^{-1} for K_{oi}^{zt} and near to zero for K^{ee}. However, these

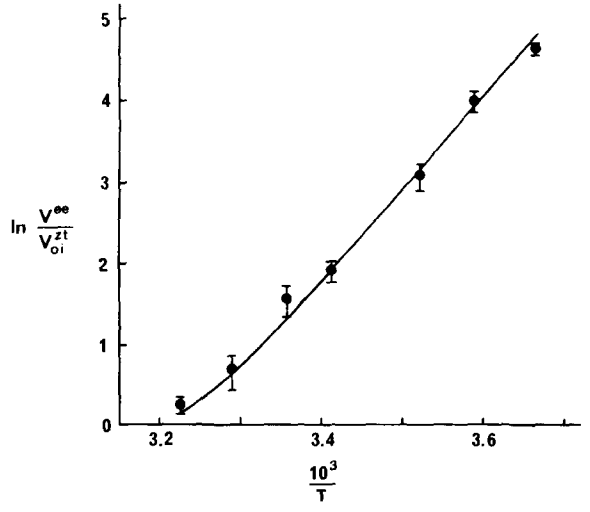

Fig. 3. The temperature-dependence of the 'trans effect' (the ratio of V^{ee} to V_{oi}^{zt}) for D-[^{14}C]glucose influx into human red cells. Measurements were made as indicated in Materials and Methods. Error bars encompass 2 S.E. The line drawn as calculated from the parameters shown in Table II.

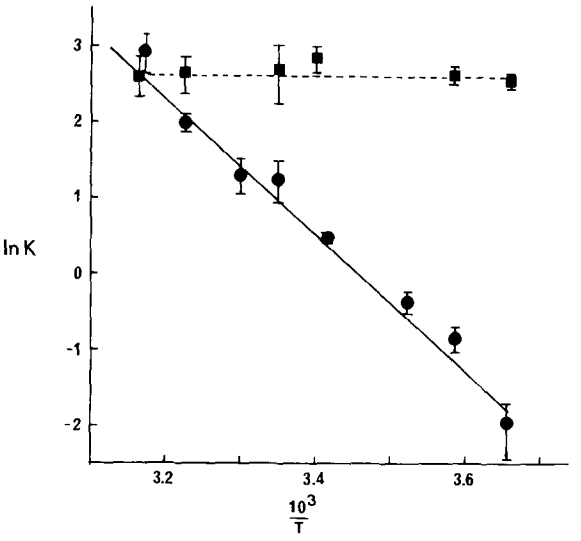

Fig. 4. A van't Hoff plot of the temperature dependences of K^{ee} and K_{oi}^{zt} for influx of D-[^{14}C]glucose into human red cells. Measurements were made as indicated in Materials and Methods and Fig. 1.

measured K_m values are not true dissociation constants and consequently these apparent enthalpies have only limited physical significance.

The extent of the asymmetry of the glucose carrier mechanism can be assessed by comparing the kinetic parameters for influx and efflux of glucose measured under zero trans conditions. Previous studies of zero trans efflux of D-[^{14}C]glucose have usually used the integrated rate equation to obtain values of K_m and V_{max} from data for efflux collected during the last half or third of the time-course of glucose exit [12,13]. Studies of this type have yielded unexpectedly high values for K_{io}^{zt}, which seem to be at variance with the predictions of the Haldane relationship, which predicts that

$$\frac{V^{ee}}{K^{ee}} = \frac{V_{oi}^{zt}}{K_{oi}^{zt}} = \frac{V_{io}^{zt}}{K_{io}^{zt}}$$

In contrast, both Miller [6] and Brahm [5] have reported substantially lower values for K_{io}^{zt} calculated from initial rates of D-[^{14}C]glucose efflux. In view of this discrepancy we made additional measurements of initial rates of D-[^{14}C]glucose efflux using our new automated syringe apparatus (Fig. 5). The values of K_{io}^{zt} obtained agree much more closely with the previous initial rate studies, rather

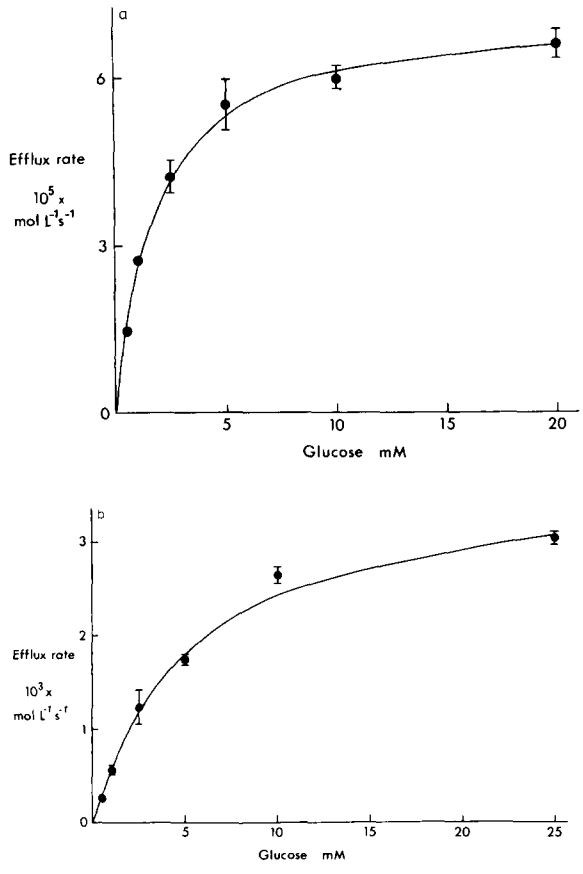

Fig. 5. The concentration-dependences of the initial rate of D-[^{14}C]glucose efflux from human red cells into glucose-free medium at 0°C (a) and 22°C (b). Experiments were carried out as described in Materials and Methods with 4–8 data points at each glucose concentration. Error bars are ±2 S.E. Values of K_{io}^{zt} and V_{io}^{zt} (calculated by non-linear regression) are 1.64 ± 0.125 mM 0.0713 ± 0.00148 mmol·l^{-1}·s^{-1} at 0°C and 5.11 ± 0.343 mM and 3.71 ± 0.092 mmol·l^{-1}·s^{-1} at 22.3°C. Lines drawn were calculated from these parameters.

than with results of analyses using the integrated rate equation, and furthermore comparison of results obtained at or near to these temperatures (Table I) under conditions of equilibrium exchange influx and zero trans influx and efflux indicates a satisfactory agreement with the Haldane relationship. It is also clear that the extent of asymmetry, as measured by the ratio of K_m for efflux and influx under zero trans conditions decreases from about 12 at 0°C to about 3 at 20°C.

In view of the discrepancy between our results for zero trans efflux of D-[^{14}C]glucose and those found previously using the integrated rate equation, we also carried out zero trans efflux experiments measuring the whole time-course of D-[^{14}C]glucose efflux at both 0°C and 20°C. Application of the integrated rate equation to these data indicated values for K_{io}^{zt} of 9.4 ± 1.2 mM at 0°C and 17.6 ± 4.2 mM at 22°C, these values being substantially higher than those indicated by our initial rate studies, but in better agreement with the measurements of Baker and Naftalin [12] at 2°C and Karlish et al. [13] at 20°C. It therefore appears that the K_{io}^{zt} obtained is very much dependent on the experimental method used.

The cause of the observed differences between initial rate and integrated rate equation analyses of glucose efflux is not known with certainty, but there are at least two possible contributary factors. Firstly, calculations based on integrated rate data depended heavily on data from the last one third of the efflux process and are consequently strongly influenced by the value taken for the final (equilibrium) D-[^{14}C]glucose content of the cells [14]. This can be easily underestimated if insufficient time is allowed for completion of isotope efflux, or

TABLE I

MEASURED VALUES OF K_m AND V_{max} FOR GLUCOSE TRANSPORT AND THE HALDANE RELATIONSHIP

All values are given ±S.E. Where necessary, measurements made near to 0 or 20°C have been corrected according to the observed temperature-dependences of the parameters.

	Temperature	
	0°C	20°C
Michaelis constants (mM)		
K_{io}^{zt}	1.64 ± 0.125	4.58 ±0.307
K_{oi}^{zt}	0.145 ± 0.0390	1.60 ±0.094
K^{ee}	12.8 ± 0.65	17.0 ±3.00
V_{max} (mmol·l^{-1}·s^{-1})		
V_{io}^{zt}	0.0713 ± 0.0148	2.57 ±0.092
V_{oi}^{zt}	0.00548 ± 0.00038	0.871 ±0.0282
V^{ee}	0.563 ± 0.0150	5.88 ±0.670
Ratios		
K_{io}^{zt} : K_{oi}^{zt}	12.1 ± 3.37	2.9 ±0.26
V_{io}^{zt} : V_{oi}^{zt}	15.0 ± 3.31	3.0 ±0.14
K^{ee} : K_{oi}^{zt}	94.0 ±25.7	10.6 ±1.96
V^{ee} : V_{oi}^{zt}	102.7 ± 7.1	6.8 ±0.80
K^{ee} : K_{io}^{zt}	7.8 ± 0.72	3.7 ±0.70
V^{ee} : V_{io}^{zt}	7.9 ± 1.65	2.3 ±0.27

overestimated if significant metabolism of D-[^{14}C]glucose occurs during the experiment. Secondly, Faust [15] has reported that the red cell glucose carrier transports β-D-glucose at a rate greater than α-D-glucose, so that when a complete time-course of glucose efflux is observed the early outflow will be predominantly β-D-glucose and the later outflow will be mainly α-D-glucose. Carruthers and Melchior [16] were unable to detect significant differences between the V_{max} and K_m for transport of α- and β-D-glucose, but their ranges of measured values for these parameters were too large to exclude a possible undetected difference. Neither of these potential sources of error is applicable when initial rates of D-[^{14}C]glucose efflux are measured.

Kinetic model

We have been able to obtain a fairly complete kinetic description of the mechanism of red cell glucose carrier using the following conventional model

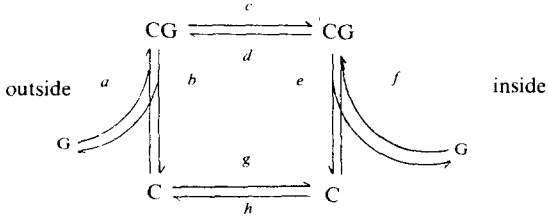

and making the assumption that glucose association with and dissociation from the carrier on both sides of the membrane is diffusion-limited and hence that rate constants a,b, e and f are very much larger than those governing reorientation of the carrier between the two sides ofthe membrane (c, d, g and h). The equations describing this model (Geck [17], Lieb and Stein [18]) then simplify to the following:

$$V^{ee} = \frac{[C]}{(1/c + 1/d)} \quad V_{oi}^{zt} = \frac{[C]}{(1/c + 1/h)} \quad V_{io}^{zt} = \frac{[C]}{(1/d + 1/g)}$$

with the temperature-dependences of the various K_m and V_{max} being governed by the activation energies of their constituent rate constants. [C] is the concentration of carrier molecules per litre cell water. Clearly, curved Arrhenius plots will result from such equations when the rate constants governing, for instance, V^{ee} have different activation energies.

We used the following procedure to fit our data to these equations.

Stage (i)

(a) Rate constant h at 0°C was estimated according the value of V_{oi}^{zt} at this temperature and rate constant c was estimated as $1000 \times h$.

(b) The activation energies for h and c were estimated from the slopes of the two extremes of the Arrhenius plot for V_{oi}^{zt}.

(c) These estimates were used as starting points for obtaining best fits of h, c and their activation energies by nonlinear regression, using the program, NONLINEAR, from the Statistical Package for the Social Sciences on the University of Manchester mainframe computer.

Stage (ii)

(a) Rate constant c and its activation energy were set to the value from stage (i)c, and rate constant d and its activation energy were set according to data obtained for V^{ee}.

(b) These estimates were used as starting points in order to find best fits for c, d and their activation energies by non-linear regression. Fitted values of c and its activation energy from stages (i) and (ii) were consistent with each other.

Stage (iii)

Non-linear regression was used to find best fit values for c, d, g, h and their respective activation energies by simultaneous analysis of the combined data for V^{ee}, V_{oi}^{zt} and V_{io}^{zt} throughout the temperature range studied. Initial estimates for c, d, h and their activation energies were those obtained from stages (i) and (ii) and initial values of g and its activation energy were estimated from values of V_{io}^{zt} measured at 0 and 22°C. Data points were weighted in accordance with the estimated S.E.

This fitting procedure led to the values of rate constants c, d, g, h and their rate constants shown in Table II. Using these values the dissociation constant for binding of glucose to the outward-facing carrier (K_s(out)) was calculated from the measured values of K^{ee}, K_{oi}^{zt}, and K_{io}^{zt} as indicated in Table III.

TABLE II

FITTED VALUES OF THE RATE CONSTANTS GOVERNING GLUCOSE TRANSPORT AND THEIR ACTIVATION ENERGIES

Rate constants have been calculated assuming that the concentrationof glucose carrier molecules [C] in human red blood cells at 100% haematocrit is 6.67 μM [3]. Values are given ± S.E.

Parameter	Rate constant × [C] ($mmol \cdot l^{-1} \cdot s^{-1}$) (0°C)	Rate constant (s^{-1}) (0°C)	Activation energy ($J \cdot mol^{-1}$)
c	8.42 ± 3.29	1113 ± 494	31700 ± 5110
d	0.602 ± 0.0231	90.3 ± 3.47	88000 ± 6170
g	0.0809 ± 0.0654	12.1 ± 0.98	127000 ± 4780
h	0.00484 ± 0.000332	0.726 ± 0.498	173000 ± 3100

These calculations indicate that the temperature-dependence of the dissociation constant of the outward-facing carrier-glucose complex is relatively small with, perhaps, a slight tendency to decrease with increasing temperature according to calculations based on K_{oi}^{zt}. The asymmetry of affinities of the carrier for glucose at the two sides of the membrane can also be calculated from the relationship

$$K_s(\text{out})/K_s(\text{in}) = (hc)/(dg)$$

and, as shown in Fig. 6, this ratio varies from 0.74 at 0°C to 0.34 at 50°C. This relatively small asymmetry of affinities contrasts with the uneven distribution of outward and inward facing carriers and carrier-glucose complexes, which are given by the ratios c/d and g/h. As shown in Fig. 6, the proportion of outward-facing unloaded carriers increases from 5.64% at 0°C to 57.3% at 50°C, while the proportion of outward-facing carrier-glucose complexes increases from 7.49% at 0°C to 79.0% at 50°C.

Overall, our analysis shows that the apparently complex kinetic properties of the red-cell glucose transport mechanism can be described satisfactorily by the conventional carrier model in which transitions of the carrier and carrier-glucose complex between inward and outward-facing confor-

TABLE III

DISSOCIATION CONSTANT, b/a

Values of the dissociation constant (b/a) for the glucose-carrier complex at the external membrane site calculated from the measured values of K_{oi}^{zt}, K_{io}^{zt}, K^{ee} and the fitted values (Table II) of c, d, g and h. All values are in mM.

$$b/a = K_{oi}^{zt} \cdot \left(\frac{1+(c/h)}{1+(g/h)}\right) = K_{io}^{zt} \cdot \frac{hc}{dg} \cdot \left(\frac{1+(d/g)}{1+(h/g)}\right) = K^{ee} \cdot \left(\frac{1+(c/d)}{1+(g/h)}\right)$$

Temperature (°C)	K_{oi}^{zt}	b/a	K_{io}^{zt}	b/a	K^{ee}	b/a
0 to 0.5	0.148	12.6	1.64	9.7	12.8	9.6
6	0.433	14.8			13.8	9.2
11	0.69	11.1				
20 to 22	1.60	7.1	5.11	6.2	17.0	10.6
25.5	3.47	7.5				
30 to 31	3.66	4.8			14.7	9.1
37	7.24	5.6			13.95	8.8
43					13.5	9.2
45	19.6	12.3				
Mean		9.5		7.9		9.5

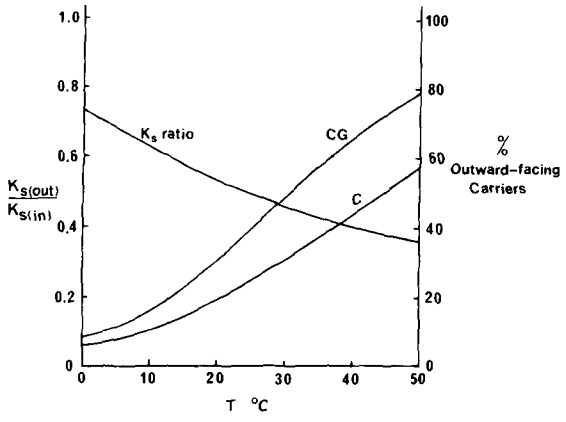

Fig. 6. The asymmetry of affinities of the outward- and inward-facing glucose carriers ($K_s(out)/K_s(in) = hc/dg = bf/ae$) and the proportions of outward facing carriers (C) and carrier glucose complexes (CG) as a function of temperature. Values plotted are calculated from the fitted values of rate constants, c, d, g and h given in Table II.

mations are governed by four rate constants of differing magnitudes and temperature dependences. It is notable, however, that despite the large differences (at 0°C) between the rate constants governing carrier movements, the dissociation constants for the carrier-glucose complex on the two sides of the membrane differ by relatively little. This finding seems satisfactory on purely physical considerations because it would be surprising if there were very large changes in the binding site for glucose in the two carrier conformations. However, as shown by Barnett et al. [19], the C4-hydroxyl of the glucose molecule may carry large (sterically hindering) groups when bound to the carrier at the outside, but similar groups inhibit binding at the inside of the cell. This change in the steric restriction for binding may account for the up to 3-fold change in affinity for glucose between inside and outside.

The comparative lack of temperature-dependence of the dissociation constants for glucose binding demands some explanation since, for most complexes, dissociation constants increase fairly markedly with temperature. Levine et al. [20] pointed out, however, that binding of glucose to the carrier is probably dependent on dissociation of water molecules bound to the glucose so that the Gibbs energies of the glucose-binding and water-dissociation processes may be similar. Possibly hydrogen bonds between glucose and associated water molecules in the aqueous solution are replaced by similar numbers of hydrogen bonds between glucose and the carrier molecule. Such hydrogen bonds could possibly provide a kinetically favoured pathway for the transition between the outward and inward-facing forms of the carrier, and hence provide a means by which glucose accelerates the rate of interchange between the two conformations at low temperatures.

Acknowledgement

This work was supported by a grant from the Wellcome Trust.

References

1 Baldwin, S.A., Baldwin, J.M. and Lienhard, G.E. (1982) Biochemistry 21, 3836–3842
2 Shanahan, M.F. (1982) J. Biol. Chem. 257, 7290–7293
3 Appleman, J.R. and Lienhard, G.E. (1985) J. Biol. Chem. 260, 4575–4578
4 Mueckler, M., Caruso, C., Baldwin, S.A., Panico, M., Blench, I., Morris, H.R., Allard, W.J., Lienhard, G.E., Lodish, H.F. (1985) Science 229, 941–945
5 Brahm, J. (1984) J. Physiol. 339, 339–354
6 Miller, D.M. (1971) Biophys. J. 11, 915–923
7 Lowe, A.G. and Walmsley, A.R. (1985) Anal. Biochem. 144, 385–389
8 Lymm, R.W., Gibson, G.H. and Hanacek, J. (1971) Rev. Sci. Instr. 42, 356–358
9 Lacko, L., Wittke, B. and Kromphardt, H. (1972) Eur. J. Biochem. 25, 447–454
10 Hankin, B.L. and Stein, W.D. (1972) Biochim. Biophys. Acta 288, 127–136
11 Lacko, L., Wittke, B. and Geck, P. (1973) J. Cell. Comp. Physiol. 82, 213–218
12 Baker, G.F. and Naftalin, R.J. (1979) Biochim. Biophys. Acta 550, 474–484
13 Karlish, S.J., Lieb, W.R. and Stein, W.D. (1972) Biochim. Biophys. Acta 255, 126–132
14 Wharton, C.W. (1983) Trans. Biochem. Soc. 11, 817–825
15 Faust, R.G. (1960) J. Cell. Comp. Physiol. 56, 103–121
16 Carruthers, A. and Melchior, D.L. (1985) Biochemistry 24, 4244–4250
17 Geck, P. (1971) Biochim. Biophys. Acta 339, 462–472
18 Lieb, W.R. and Stein, W.D. (1974) Biochim. Biophys. Acta 373, 178–196
19 Barnett, J.E.G., Holman, G.D., Chalkley, R.A. and Munday, K.A. (1975) Biochem. J. 135, 211–221
20 Levine, M., Levine, S. and Jones, M.N. (1971) Biochim. Biophys. Acta 225, 291–300